Improving the Performance of a 300 MW Down-Fired Pulverized-Coal Utility Boiler by Inclining Downward the F-Layer Secondary Air

ARTICLE *in* ENERGY & FUELS · SEPTEMBER 2010

Impact Factor: 2.79 · DOI: 10.1021/ef1005868

5 AUTHORS, INCLUDING:

Huaichun Zhou
Tsinghua University
148 PUBLICATIONS **1,193** CITATIONS

Energy Fuels **2010,** *24,* 4857–4865 · DOI:10.1021/ef1005868
Published on Web 08/23/2010

energy&fuels
article

Improving the Performance of a 300 MW Down-Fired Pulverized-Coal Utility Boiler by Inclining Downward the F-Layer Secondary Air

Qingyan Fang,[†] Huajian Wang,[†] Huaichun Zhou,*[,†] Lin Lei,[‡] and Xuelong Duan[‡]

[†]*State Key Laboratory of Coal Combustion, Huazhong University of Science and Technology, Wuhan 430074, People's Republic of China, and* [‡]*Hunan Electric Power Test and Research Institute, Changsha 410007, People's Republic of China*

Received May 9, 2010. Revised Manuscript Received August 2, 2010

This paper presents a systematic study on improving the performance of a 300 MW down-fired pulverized-coal utility boiler by inclining downward the F-layer secondary air (SA). A numerical method was adopted to evaluate the effects of inclined angles on the characteristics of flow, combustion, and nitrogen oxide (NO_x) emissions in the furnace. Retrofitting was conducted to incline the F-layer SA downward with an optimal inclined angle of 25°. Full-scale experimental measurements were carried out before and after retrofitting. The results indicate that inclining downward the F-layer SA can increase the flame penetration depth and lower downward the flame center. The residence time of pulverized-coal particles increases, and the SA staging level enhances in the furnace. The boiler performance is improved with absolute increases of 3.55, 3.31, and 2.20% in boiler efficiencies and relative reductions of 28.65, 19.07, and 12.53% in NO_x emissions under 300, 240, and 190 MW loads, respectively.

1. Introduction

Low carbon energy requires a higher performance for fuel-usage equipment to reduce carbon emissions, as well as other pollution emissions. The down-fired boilers, being able to achieve stable combustion and reasonable coal burnout, are suitable to burn low volatile coals, such as anthracite in power plants.[1] Currently, more than 100 down-fired boilers, having a total capacity of approximately 41 000 MW, are either in service or under construction in China. To better understand the combustion characteristics in down-fired boilers, several studies have been carried out in recent years.[2−7] However, practical operation of down-fired boilers suffers from the problems of high carbon contents in fly ash, high nitrogen oxide (NO_x) emissions,[2,3] and serious slagging,[4] especially when burning low-quality coals. For one thing, because of the low ignitability and reactivity of the coal burned, the ignition and burnout of pulverized coal are delayed.[3] Also, a small momentum ratio of arch- to wall-injected secondary air (SA) leads to a short flame depth in the lower furnace.[5] Therefore, both the residence time of pulverized-coal particles and SA staging level are deficient, resulting in high carbon contents in fly ash and high NO_x emissions.

In the case of unchanging the coal properties, there are two methods to improve the deficiencies above. One is increasing the arch-injected SA, which can increase the momentum ratio of the arch- to wall-injected SA. This can normally increase the flame penetration depth in the lower furnace and achieve a low flame operating mode, which is helpful in reducing both carbon contents in fly ash and NO_x emissions.[5] However, it may lead to ignition deterioration, unstable combustion, or even fire extinguishing when low-quality coals are fired. Therefore, the low velocities of the arch-injected primary air (PA) and SA are often adopted by operators to ensure stable combustion in the furnace.

The other one is inclining downward the horizontally wall-injected F-layer SA, which can effectively increase the momentum ratio of the arch- to wall-injected SA and the flame penetration depth without a negative influence on the ignition and combustion of pulverized coal. Li et al.[8,9] performed the experimental investigations on the effects of the inclined F-layer SA on the gas/particle flow and combustion characteristics on a small-scaled furnace and a full-scale down-fired boiler burning the designed coal, respectively. Both the penetration depths of the arch-injected air and particles increase with increasing the inclined angle. The carbon content in the fly ash decreases 37.38%, and NO_x emission decreases 8.33%. However, it is difficult from the limited experimental data to exhibit more detail on the effects of the inclined F-layer SA on the ignition and combustion characteristics in a full-scale boiler furnace. The numerical method, being able to reveal more detail on the combustion process, has been widely applied to investigate not only the pulverized-coal combustion in utility boilers[10−14] but also the blended coal combustion in

*To whom correspondence should be addressed. Fax: +86-27-87540249. E-mail: hczhou@mail.hust.edu.cn.

(1) Garcia-Mallol, J. A.; Kukoski, A. E.; Winkin, J. P. Anthracite firing design for central stations: Ignition and emissions aspects. *Proceedings of the International Pittsburgh Coal Conference*; Taiyuan, China, 1997.
(2) Ren, F.; Li, Z. Q.; Zhang, Y. B.; Sun, S. Z.; Zhang, X. H.; Chen, Z. C. *Energy Fuels* **2007**, *21*, 668–676.
(3) Li, Z. Q.; Ren, F.; Zhang, J.; Zhang, X. H.; Chen, Z. C.; Chen, L. Z. *Fuel* **2007**, *86*, 2457–2462.
(4) Fang, Q. Y.; Wang, H. J.; Wei, Y.; Lei, L.; Duan, X. L.; Zhou, H. C. *Fuel Process. Technol.* **2010**, *91*, 88–96.
(5) Fueyo, N.; Gambon, V.; Dolazo, C.; Gonzalez, J. F. *J. Eng. Gas Turbines Power* **1999**, *121*, 735–740.
(6) Fan, J. R.; Zha, X. D.; Cen, K. F. *Fuel* **2001**, *80*, 373–381.
(7) Fan, J. R.; Liang, X. H.; Chen, L. H.; Cen, K. F. *Energy* **1998**, *23*, 1051–1055.
(8) Li, Z. Q.; Ren, F.; Chen, Z. C.; Liu, G. K.; Xu, Z. X. *Energy Fuels* **2009**, *23*, 5846–5854.
(9) Li., Z. Q.; Ren, F.; Chen, Z. C.; Chen, Z.; Wang, J. J. *Fuel* **2010**, *89*, 410–416.
(10) Xu, M, H.; Azevedo, J. L. T.; Carvalho, M. G. *Fuel* **2000**, *79*, 1611–1619.

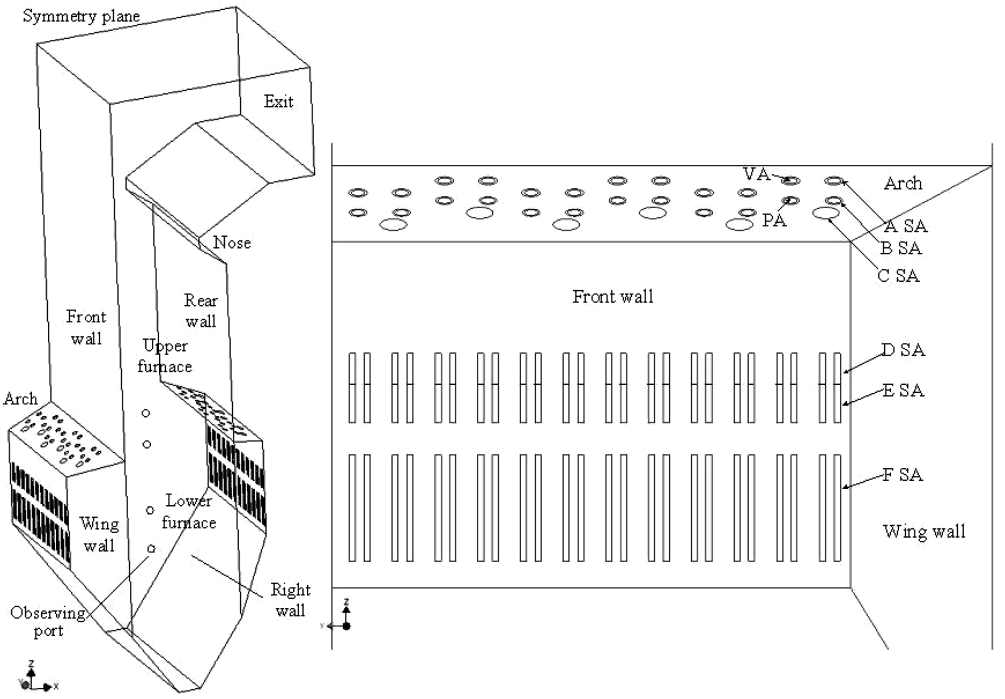

Figure 1. Schematic diagram of the boiler (only half of the boiler is shown in the figure because the furnace structure is symmetrical) (PA, primary air; VA, vent air; SA, secondary air).

blast furnaces,[15] biomass combustion,[16,17] and oxy-fuel combustion.[18,19] However, no numerical study has been reported thus far on the inclined F-layer SA in a down-fired boiler. This work conducts a systematic study on improving the performance of a 300 MW down-fired pulverized-coal utility boiler by inclining downward the F-layer SA. A numerical method is adopted to exhibit more detail on the effects of the inclined angles on the combustion characteristics of the boiler.

2. Methodology

2.1. Study Object. The study object is a 300 MW down-fired pulverized-coal utility boiler manufactured using the technique of the Forster Wheeler Company (see Figure 1). The zone of the furnace below the arches is the lower furnace (pulverized-coal burning zone). The zone above the arches is the upper furnace (pulverized-coal burnout zone). The dimensions of the upper furnace are $7.63 \times 24.76 \times 23.82$ m, and the dimensions of the lower furnace are $13.73 \times 24.76 \times 15.48$ m. The lower furnace is 4108 m^3 in volume with 639 m^2 of refractory coverage on the walls. A direct firing pulverized-coal preparation system is used having four ball mills. The furnace is, on the arches, equipped with 24 double-cyclone burners, which can enrich the coal/air mixture. The mixture flow of the PA and pulverized coal is divided into fuel-rich and fuel-lean streams. The fuel-rich stream is supplied downward into the lower furnace through the burner nozzle with a 5° angle between its axis and the vertical direction. The fuel-lean stream is supplied downward into the lower furnace from the vent air (VA) nozzle. SA is supplied into the furnace according to the need of staging air for gradual and complete combustion. About 70% of SA, divided into three streams D, E, and F, is horizontally supplied into the furnace through the D, E, and F nozzles under the arches. The remaining SA, divided into three streams A, B, and C, is introduced through the A, B, and C nozzles, concentric with the fuel-rich nozzle, fuel-lean nozzle, and oil igniter. The designed coal is a low-volatile coal with a volatile content of 11.22% (dry ash free) and a lower heating value of 20 990 kJ/kg (as received). The designed pulverized-coal fineness, R_{90}, is about 8%. There are some observing ports on both sidewalls along the furnace height.

2.2. Numerical Simulations. A computational fluid dynamics program, known as Fluent (version 6.3.26), was used to conduct the simulations. The calculation procedure includes numerical solution of the time-averaged conservation equations for the gas and particle phases, using the Eulerian description for the former and the Lagrangian description for the latter. The turbulence flow was simulated by the standard $k-\varepsilon$ model. A mixture fraction method with a probability density function (PDF) was used for the turbulence combustion modeling of the gas phase. The stochastic particle trajectory model was used to simulate the flow of pulverized-coal particles in the furnace. Coal devolatilization was simulated by a two-parallel-reaction model, and char particle combustion was calculated by a kinetic and diffusion model. The P1 method was used to simulate radiation heat transfer in the furnace. More detailed descriptions of these models can be found in the literature.[20]

NO_x simulation mainly considers the formation of thermal NO and fuel NO. Thermal NO is generated from the oxidation

(11) Thomas, L. B.; Francisco, C.; Sebastien, C.; Pietrzyk, S.; Blondin, J.; Baudoin, B. *Fuel* **2007**, *86*, 2213–2220.
(12) Belosevic, S.; Sijercic, M.; Stefanovic, P. *Int. J. Heat Mass Transfer* **2008**, *51*, 1970–1978.
(13) Zhao, L. L.; Zhou, Q. T.; Zhao, C. S. *Combust. Flame* **2008**, *155*, 277–288.
(14) Korytnyi, E.; Saveliev, R.; Perelman, M.; Chudnovsky, B. *Fuel* **2009**, *88*, 9–18.
(15) Shen, Y. S.; Guo, B. Y.; Yu, A. B.; Zulli, P. *Fuel* **2009**, *88*, 255–263.
(16) Ma, L.; Jones, J. M.; Pourkashanian, M. *Fuel* **2007**, *86*, 1959–1965.
(17) Yin, C. G.; Rosendahl, L.; Kær, S. K.; Clausen, S.; Hvid, S. L.; Hille, T. *Energy Fuels* **2008**, *22*, 1380–1390.
(18) Tiggesa, K. D.; Klaukea, F.; Berginsa, C.; Busekrus, K.; Niesbach, J.; Ehmann, M.; Kuhr, C.; Hoffmeister, F.; Vollmer, B.; Buddenberg, T.; Wu, S.; Kukoski, A. *Energy Procedia* **2009**, *1*, 549–556.
(19) Toporov, D.; Bocian, P.; Heil, P.; Kellermann, A.; Stadler, H.; Tschunko, S.; Förster, M.; Kneer, R. *Combust. Flame* **2006**, *155*, 605–618.
(20) Smoot, L. D.; Smith, P. J. *Coal Combustion and Gasification*; Plenum Press: New York, 1989.

of N_2 in the combustion air. The formation of thermal NO is determined by a set of strongly temperature-dependent chemical reactions. The thermal NO was simulated using a simple combined kinetic rate expression for the classical Zeldovich mechanism.[21] The partial equilibrium approach, for both the atomic oxygen and hydroxyl radical, was adopted. For the fuel NO modeling, the global models proposed by De Soete[22] are considered as the fuel NO mechanism, as shown in Figure 2. It is assumed that the fuel-bound nitrogen of the coal is distributed between the volatile and the char. The nitrogen in the volatile evolves as HCN or NH_3 intermediates, and the nitrogen in the char converts to NO directly. The advanced chemical percolation devolatilization (CPD) model with the prediction of nitrogen release,[23,24] instead of an empirical method, was adopted to predict the mass fraction of the nitrogen release in the volatile, α, and the percentage of the nitrogen in the volatile evolving as HCN intermediate, β. The model predictions show good agreement with the nitrogen release data from the experiments of different coals in various conditions. It is suitable to calculate the nitrogen release during the devolatilization of pulverized coal in the combustion condition of the studied boiler. The conversion ratio of the nitrogen in the char was taken as 0.5.[25] A β PDF was used to account for the temperature and oxygen species fluctuations on the NO formation in turbulent flows.[20]

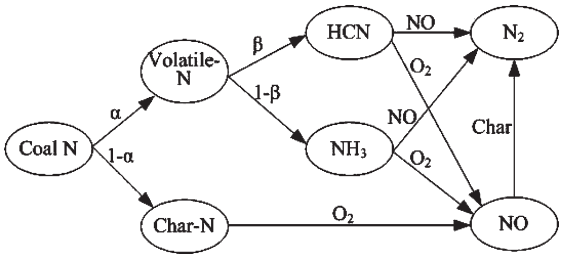

Figure 2. Schematic diagram of the fuel NO formation mechanism.

Table 1. Coal Properties

item	before retrofitting	after retrofitting
Proximate Analysis (wt %) (as Received)		
volatile matter	7.63	9.21
moisture	8.07	8.02
ash	37.38	37.63
fixed carbon	46.92	45.14
lower heating value (kJ/kg)	17436	17235
Ultimate Analysis (wt %) (as Received)		
carbon	47.99	47.13
hydrogen	2.14	2.11
oxygen	3.18	3.91
sulfur	0.56	0.59
nitrogen	0.68	0.61

Because of the symmetry of the structure and aerodynamic characteristics in the furnace, the simulations were carried out on a half-boiler furnace along the width.[4,5] A partition meshing method was adopted to achieve high-quality grid. Grid-dependent tests were performed, and a total of 1 560 000 cells was finally used. The grid was refined near the burner zone. The SIMPLE algorithm of pressure correction was applied to consider the coupling of velocity and pressure fields. Using the first-order finite difference method, the conservation equations of the gas phase were solved with successive under-relaxation iterations until the solution satisfied a pre-specified tolerance.

The simulations were carried out at the inclined angles of 0°, 15°, 25°, and 35° for the F-layer SA under 300 MW load. The 0° inclined angle means that the F-layer SA is horizontal. The simulations were also conducted to validate the availability of the adopted models at 240 and 190 MW loads before and after the retrofit of the boiler. The coal fired before the retrofit was

Table 2. Simulation Conditions

item	nozzle size	temperature (K)	velocity (m/s)	flow rate (kg/s)	air ratio (%)	coal concentration (kg/kg)
PA	Φ 0.253 m	373	21.8	44.14	14.56	0.95
VA	Φ 0.253 m	373	5.0	10.01	3.30	0.14
A SA	Φ 0.330 m	605	8.0	13.55	4.47	
B SA	Φ 0.330 m	605	10.0	14.54	4.80	
C SA	Φ 0.600 m	605	8.0	15.92	5.25	
D SA	0.30 m^2	605	5.0	18.45	6.09	
E SA	0.30 m^2	605	8.0	34.85	11.50	
F SA	0.92 m^2	605	12.5	151.63	50.03	

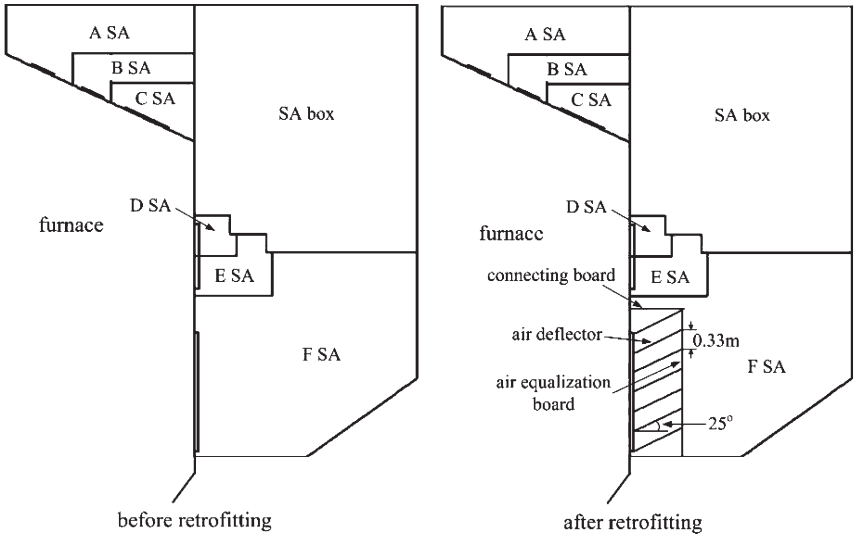

Figure 3. Schematic diagram of the retrofit for F-layer SA.

Table 3. Operating Conditions in the Six Cases[a]

item	load (MW)	SA temperature (K)	total air flow rate (km^3/h)	F SA damper opening (%)	coal feeding rate (kg/s)	R_{90} (%)	mills in service
before retrofitting	300	605	921	35	45.49	12.5	A, B, C, and D
	240	594	821	30	36.23	9.8	A, B, C, and D
	190	588	613	25	28.29	7.5	A, B, and C
after retrofitting	300	604	1032	35	45.99	11.6	A, B, C, and D
	240	595	944	30	36.61	9.5	A, B, C, and D
	190	590	732	25	28.98	8.0	A, B, and C

[a] The temperature of the PA and pulverized-coal mixture is 373 K. VA valve opening is 25% in all six cases. The damper openings of A, B, C, D, and E SA are 15, 20, 10, 10, and 15% in the six cases, respectively. The adjustable vane is located at the lowest position of the PA nozzle.

used in the simulations (see Table 1). The operating conditions for the burner are listed in Table 2. The wall function method and temperature wall were employed for the velocity and thermal boundary conditions, respectively. The size distribution of the pulverized-coal particles obeys the Rosin−Rammler algorithm, with an average diameter of 55 μm and a spread parameter of 1.26. The kinetics parameters of char combustion, the pre-exponential factor, and activation energy, are 0.016 kg m^{-2} s^{-1} Pa^{-1} and 83 700 kJ/kmol, respectively.

2.3. Full-Scale Retrofitting and Experimental Measurements. Retrofitting was conducted to incline the F-layer SA downward through the air deflectors fixed in the F SA rooms with an optimal angle after the simulations. The schematic diagram of the retrofit is shown in Figure 3. Combustion experimental measurements were conducted at 300, 240, and 190 MW loads before and after retrofitting. The properties of the coals used in the experiments are shown in Table 1. The operating conditions of all six cases are listed in Table 3. A carefully calibrated portable flame temperature measuring system using a visible flame image processing technique was employed to measure the flame temperatures along the furnace height for the two former loads. The measuring system includes a notebook computer, a video collecting card, a flame image detector, and the image processing software. It can take flame images and calculate the image temperatures in a very short time. The measuring temperature range is 500−2000 °C. The radiation images of red (R) and green (G) are obtained from the color flame image and are assumed directly proportional to the approximately monochromatic radiations at their central wavelengths of λ_r = 610.8 nm and λ_g = 510.8 nm, respectively, after a careful test of the charge-coupled device (CCD) camera used in the measurements. The flame temperature measurement is based on Planck's radiation law for blackbody radiation. A blackbody furnace with the temperature range from 1000 to 2000 K (with temperature errors within ±5 K) is used to carefully calibrate the flame image detector. The flame image temperature can be computed by the two-color method. The measuring system and method were described in more detail by Wang et al.[26] The combustion was maintained stable during the measurements. At each cross-section, the system was used to measure the temperatures through the four observing ports in turn (see Figure 4). The average temperature was then calculated to stand for the temperature level at this cross-section.

Some performance parameters, such as the boiler efficiencies and NO emissions, were measured. A MSI EURO-type flue gas analyzer was used to measure the components of flue gas. Flue gas and fly ash samplings were conducted at the flue entrance of the air preheater. The exhaust gas temperature was measured at the air preheater exit. Coal sampling was carried out at the coal hopper exits. Pulverized coal sampling was carried out using the sampling equipment installed on the pipes of primary air and pulverized-coal mixture. Bottom ash was sampled. The flow rate of desuperheater water was also recorded.

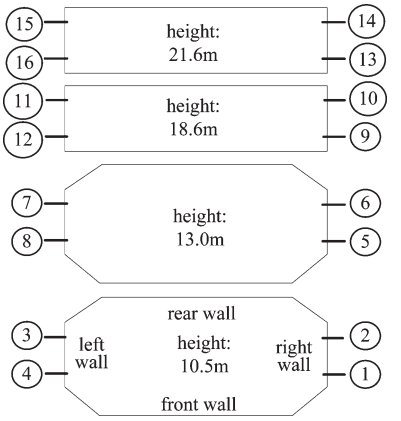

Figure 4. Measurement positions of the flame measuring system.

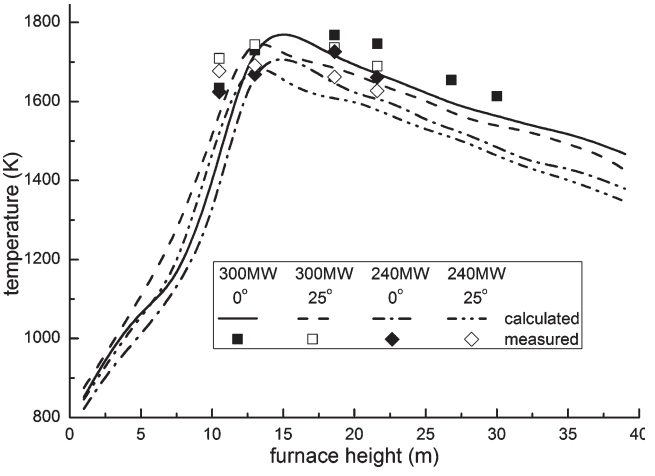

Figure 5. Comparison of the calculated and measured temperatures.

3. Results and Discussion

3.1. Validation for the Simulated Results. The highest temperatures calculated are compared to those measured in the central furnace because the temperatures measured using the two-color method are close the highest temperatures in the central furnace.[27] Figure 5 shows that the

(21) Hill, S. C.; Smoot, L. D. *Prog. Energy Combust. Sci.* **2000**, *26*, 417–458.
(22) De Soete, G. G. Overall reaction rates of NO and N_2 formation from fuel nitrogen. *Proceedings of the 15th International Symposium on Combustion*; Pittsburgh, PA, 1975.
(23) Genetti, D.; Fletcher, T. H. *Energy Fuels* **1999**, *13*, 1082–1091.
(24) Perry, S. T.; Fletcher, T. H. *Energy Fuels* **2000**, *14*, 1094–1102.
(25) Glarborg, P.; Jensen, A. D.; Johnsson, J. E. *Prog. Energy Combust. Sci.* **2003**, *29*, 89–113.
(26) Wang, H. J.; Huang, Z. F.; Wang, D. D.; Luo, Z. X.; Sun, Y. P.; Fang, Q. Y.; Lou, C.; Zhou, H. C. *Meas. Sci. Technol.* **2009**, *20*, 4006–4017.
(27) Zhou, H. C.; Han, S. D.; Zheng, C. G. *Proc. CSEE* **2002**, *22*, 109–114.

Table 4. Calculated and Measured Results in the Six Cases

item	load (MW)	carbon content of the fly ash (%)		NO (mg/m^3, 6% O_2)		O_2 content (vol %)		exhaust gas temperature (K)	boiler efficiency (%)	flow rate of desuperheater water (tons/h)
		calculated	measured	calculated	measured	calculated	measured			
before retrofitting	300	6.9	7.27	863	920	3.83	3.51	144	86.38	158
	240	5.62	6.16	692	591	4.18	3.82	141	86.64	115
	190	4.21	4.66	569	441	4.60	4.07	138	87.53	84
after retrofitting	300	4.16	5.86	793	645	3.42	4.03	136	89.93	125
	240	3.64	4.34	597	478	3.84	4.80	133	89.95	98
	190	3.02	4.12	492	385	4.31	4.85	126	89.73	76

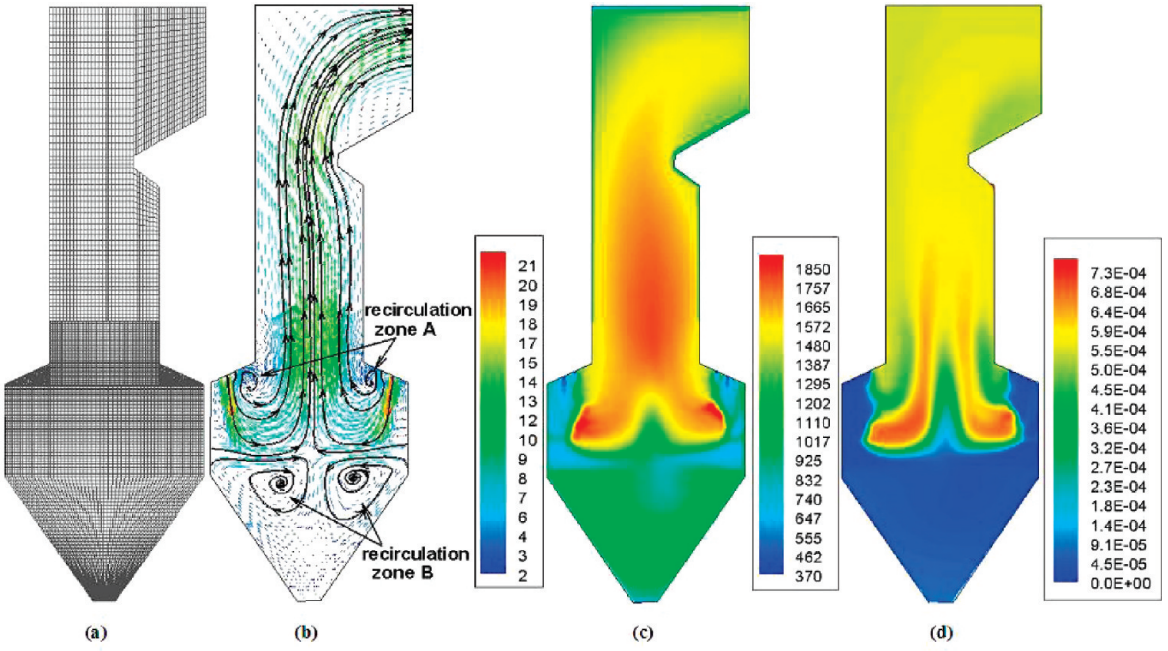

Figure 6. Central cross-section of the burner nozzle with horizontal F-layer SA: (a) grid used for computed results, (b) flow field (m/s), (c) temperature distribution (K), and (d) NO concentration distribution (10^6 ppm).

calculated temperatures are consistent with the measured values, with a maximum error of 12.56% at 10.5 m for the retrofitted case of 240 MW. During the combustion process of pulverized coal, the temperatures of pulverized-coal particles are generally higher than those of local gas, as much as 200 K.[28] The heat radiation received by the measuring system mainly comes from the high-temperature particle medium in the furnace. Therefore, the measured temperatures are higher than those calculated. The comparison of the calculated and measured values for the carbon content in the fly ash and NO emission is shown in Table 4. The calculated carbon content and NO emission show good agreement with those measured with 9.77 and 6.30% errors at 300 MW before retrofitting. The calculated results can properly reveal the variation characteristics of the carbon contents and NO emissions after retrofitting, although the calculation errors increase in some cases. These indicate that the models adopted in the present study are suitable for investigating the effects of the inclined angles on the combustion characteristics of the boiler.

Figure 6 shows the grid, flow field, temperature, and NO concentration distributions over the central cross-section of the burner nozzle at the 0° inclined angle (horizontal F-layer SA). The flow field (see Figure 6b) presents a W shape, properly reflecting the practical aerodynamic characteristics in the down-fired boiler. There exist two recirculation zones, A, below the arches. They can entrain high-temperature flue gas, enhance the heat transfer between the pulverized-coal particles and high-temperature flue gas, and thus, be favorable for the stable ignition and combustion of the pulverized coal. In the ash hopper, there also exist two very large recirculation zones, B, which can demonstrate the penetration depth of the arch-injected air in the lower furnace. The larger recirculation zone B means a shorter penetration depth. Because of the low ignitability of the coal used, the ignition of the arch-injected PA and pulverized-coal mixture is far away from the burner nozzle (see Figure 6c). This is consistent with the reported result.[3] After being ignited, the pulverized coal intensely burns and releases a great amount of heat, producing a high-temperature zone in the lower furnace. These are favorable conditions for the stable ignition, combustion, and burnout of the low-volatile coal. The NO formation is mainly in the lower furnace, and the maximum NO concentration is located near the position behind the ignition point. Because of its reduction by the char, the NO gradually decreases along the furnace height (see Figure 6d).

(28) Field, M. A. *Combust. Sci. Technol.* **1969**, *13*, 237–251.

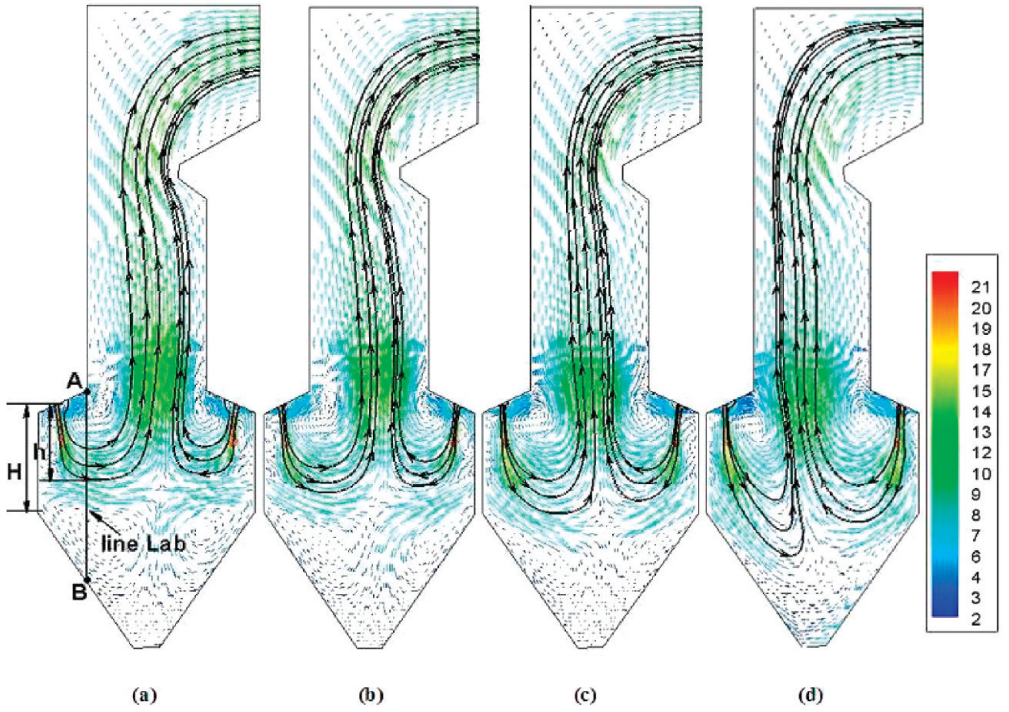

Figure 7. Comparison of the flow fields (m/s) at different inclined angles: (a) 0°, (b) 15°, (c) 25°, and (d) 35°.

Table 5. Simulated Results under the Different Inclined Angles

item	0°	15°	25°	35°
momentum ratio of arch- to wall-injected air	0.62	0.86	1.05	1.29
dimensionless penetration depth of arch-injected air	0.67	0.78	0.95	1.23
recirculation zone length (m)	1.424	1.751	1.842	2.022
recirculation heat (kJ)	832	1229	1652	2227
ignition distance (m)	2.968	2.751	2.573	2.309
dimensionless flame depth	0.75	0.87	0.99	1.25
average residence time of coal particles (s)	5.94	6.34	6.73	6.96
carbon content in the fly ash (%)	6.90	5.56	4.16	2.52
NO emission (mg/m^3, 6% O_2)	863	824	793	760
O_2 at the exit (vol %)	3.83	3.64	3.42	3.17
average temperature at the nose (K)	1488	1468	1450	1442

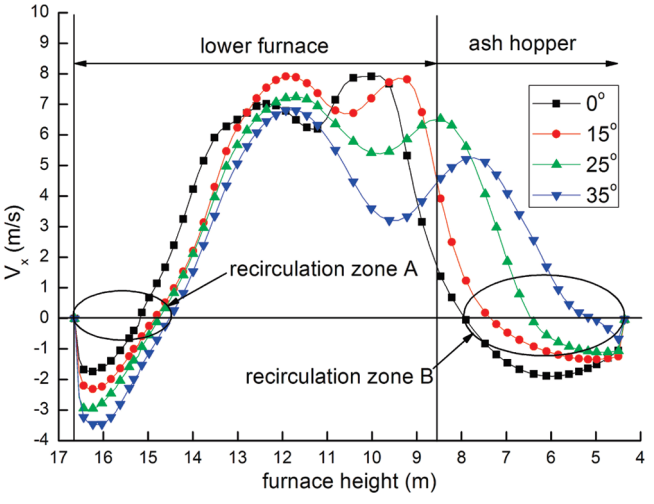

Figure 8. Comparison of the *x*-direction velocity distributions along line Lab for the different inclined angles.

3.2. Effects of the Inclined Angles on the Boiler Characteristics. Figure 7 presents the comparison of the flow fields for the different inclined angles over the central cross-section of the burner nozzle. As the inclined angle increases, the momentum ratio of the arch- and wall-injected air increases, as shown in Table 5. The penetration depth of the arch-injected air flow increases in the lower furnace, and the recirculation zone B decreases. The dimensionless penetration depths of the arch-injected air in the lower furnace can be calculated by h/H, where h is the penetration depth of the arch-injected air in the lower furnace and H is the distance from the burner nozzle to the ash hopper top. It increases with increasing the inclined angle (see Table 5). This can increase the residence time of the pulverized-coal particles, being favorable to increase the pulverized-coal burnout. However, the arch-injected air flow directly penetrates into the ash hopper at 35°. This may bring a tendency of slagging on the ash hopper walls.

With increasing the inclined angle, the recirculation zone A enlarges, being able to entrain more high-temperature flue gas. It is helpful in improving the ignition and combustion of the pulverized coal. The *x*-direction velocity distribution on line Lab is used to quantify the length and velocity of the recirculation zone A (see Figure 8). The length of the recirculation zone A increases with increasing the inclined angle. The bigger the inclined angle, the longer the length (see Table 5). The recirculation heat Q along the central cross-section of

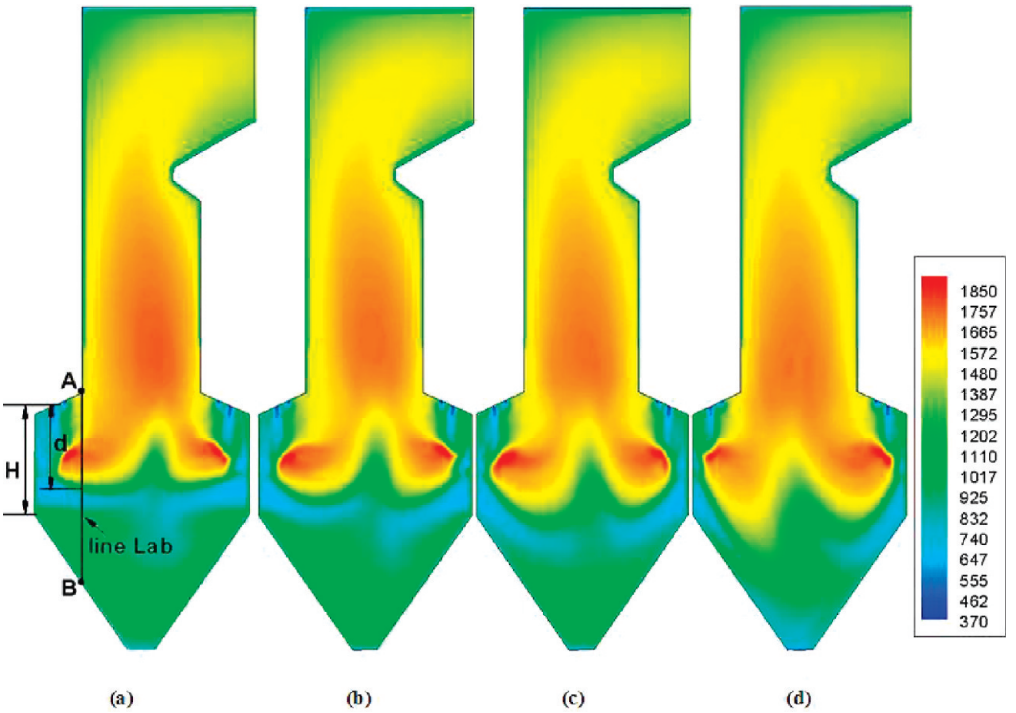

Figure 9. Comparison of the temperature distributions (K) for the different inclined angles: (a) 0°, (b) 15°, (c) 25°, and (d) 35°.

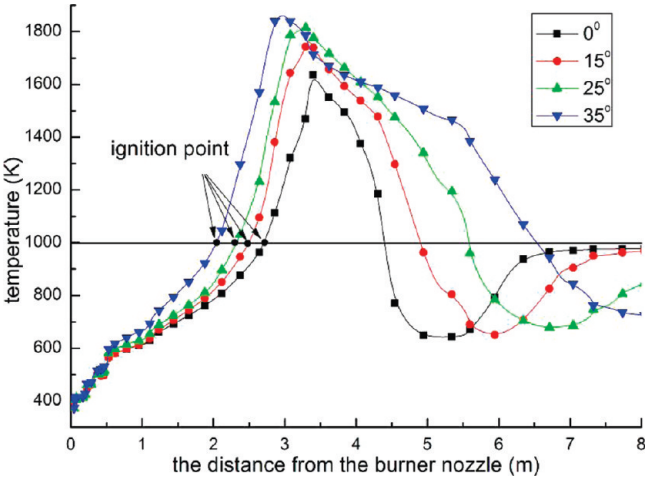

Figure 10. Comparison of the temperature distributions along the PA nozzle axis of the burner for the different inclined angles.

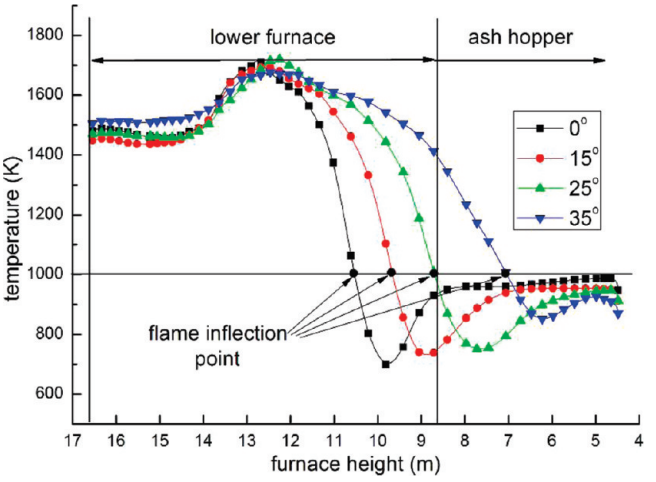

Figure 11. Comparison of the temperature distributions along line Lab for the different inclined angles.

the burner nozzle can be calculated in the recirculation zone A by the following equation:

$$Q = \int_0^l C_{p_{gas}} v_x \rho_{gas} T_{gas} \mathrm{d}l \qquad (1)$$

where $C_{p_{gas}}$ is the flue gas specific heat capacity, v_x is the recirculation velocity, ρ_{gas} is the flue gas density, T_{gas} is the flue gas temperature, and l is the recirculation zone length. They can be obtained by the simulations. The calculated results are shown in Table 5. The recirculation heat increases with increasing the inclined angle.

Figure 9 shows the comparison of the temperature distributions for the different inclined angles. With increasing the inclined angle, both the penetration depth and fullness of the flame in the lower furnace increase. The comparison of the temperature distributions along the PA nozzle axis is shown in Figure 10 for the different inclined angles. As the inclined angle increases, the temperature in the early stage increases more rapidly. Temperature peak increases and the temperature peak point also shifts toward the nozzle along the axis. It indicates that the ignition and combustion of the pulverized coal are closer to the burner nozzle. This is very helpful in improving the ignition and combustion characteristics. By defining the position of 1000 K on the nozzle axis as the ignition point of the PA and pulverized-coal mixture,[29] the ignition distance is quantified, as shown in Table 5. The ignition distance shortens with increasing the inclined angles. This is due to the more recirculation heat entrained by the larger recirculation zone A, as well as the stronger radiative heat by the higher temperature flame in the lower furnace.

(29) Gera, D.; Mathur, M.; Freeman, M. *Energy Fuels* **2003**, *17*, 794–795.

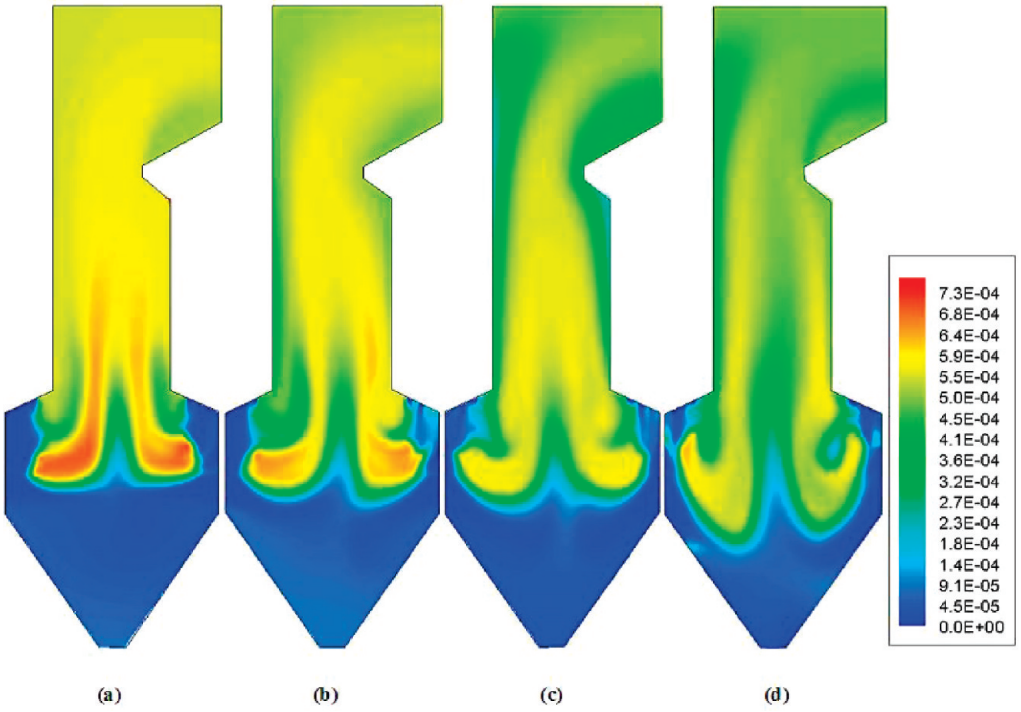

Figure 12. Comparison of the NO concentration distributions (10^6 ppm) for the different inclined angles: (a) 0°, (b) 15°, (c) 25°, and (d) 35°.

The comparison of the temperature distributions along line Lab is shown in Figure 11 for the different inclined angles. By defining the position of 1000 K on line Lab as the flame inflection point in the lower furnace, the dimensionless flame depth in the lower furnace can be calculated by d/H, where d is the flame depth in the lower furnace and H is the distance from the burner nozzle to the ash hopper top. As the inclined angle increases, the dimensionless flame depth increases and the residence time of the pulverized-coal particles in the high-temperature flame increases. Consequently, the carbon content in the fly ash decreases and the pulverized-coal burnout increases (see Table 5). The flame just fills the lower furnace at 25°. However, at 35°, the flame with high-temperature particles has penetrated into the ash hopper, which may lead to a strong tendency of slagging on the ash hopper walls. Because of the inertial effect of the pulverized-coal particles, the dimensionless flame depths are bigger than those of the arch-injected air flows.[8]

Figure 12 shows the comparison of the NO concentration distributions for the different inclined angles. Because of the highly centralized combustion, the NO formation centralizes in the lower furnace at 0°. With increasing the inclined angle, the zone with NO formation expands because of the decrease in the ignition distance and the increase in the flame penetration depth. The maximum NO concentration gradually reduces. This is because the inclined angle delays the mixing of the flame and F-layer SA and enhances the SA staging level during the pulverized-coal combustion, prolonging the residence time for combustion in a lean-oxygen atmosphere and restraining the formation of fuel NO. At the same time, the NO concentration along the furnace height also decreases because the path for NO reduction by the char increases. Therefore, the NO emission decreases with increasing the inclined angle (see Table 5).

With increasing the inclined angle, the average temperature at the furnace nose gradually decreases (see Table 5). It can improve the characteristics of heat transfer in the top furnace as well as the tail sections and reduce the desuperheater water flow rate and exhaust gas temperature. On the basis of the analysis above, it can be concluded that 25° is an optimal inclined angle for the F-layer SA. In comparison to the results at 0° (the horizontal F-layer SA), the ignition distance reduces 13.31% and the flame depth in the lower furnace increases 32.0% at 25°. The carbon content in the fly ash reduces 39.70%. The NO emission decreases 8.11%. The boiler performance can be improved without the tendency of slagging on the ash hopper walls.

3.3. Full-Scale Experimental Results. Figure 5 shows the measured average temperatures along the furnace height at 300 and 240 MW. In general, the pulverized-coal particles are mainly fired in the lower furnace (the burning zone) and the temperature peak or the flame center is located in the lower furnace. However, it can be found that, before retrofitting, the maximum temperatures are both at 18.6 m, above the furnace arches. This indicates that the flame center shifts upward. On one hand, because of the low ignitability and reactivity of the coal used, the ignition and combustion of the pulverized-coal are delayed. On the other hand, a small momentum ratio of the arch- to wall-injected air results in a short flame depth in the lower furnace. After retrofitting, the lower furnace temperatures increase. The temperatures at 13.0 m (below the furnace arches) are both higher than those at 18.6 m. These indicate that the flame center shifts downward into the lower furnace and the flame penetration depth increases.

The measured performance parameters are all shown in Table 4 for the six cases. In comparison to the results before retrofitting, both the carbon contents in the fly ash and exhaust gas temperatures decrease after retrofitting. The boiler efficiencies increase 3.55, 3.31, and 2.20% in the absolute values and the NO emissions decrease 28.6, 19.07, and 12.6% at 300, 240, and 190 MW, respectively. The percentages for NO emission reduction are more than those by the simulations. For one thing, the coal burned after

retrofitting has more volatile content and can release more fuel nitrogen during the devolatilization, being favorable to reduce more NO formed in the early stage of the pulverized-coal combustion. Additionally, the coal used after retrofitting has less nitrogen content, reducing the formation of fuel NO. These are also the reasons why the NO emissions in the present study are much less than those reported by Li et al.[3] and Fuyeo et al.[5] The flow rates of desuperheater water decrease 20.89, 14.78, and 9.52% under the three loads. The flue gas O_2 contents at the furnace exit also increase without any negative influence on the ignition and combustion.

4. Conclusions

A systematic study was conducted to improve the performance of a 300 MW down-fired pulverized-coal utility boiler by inclining downward the F-layer SA. A numerical method was adopted to evaluate the effects of the inclined angle on the combustion characteristics. As the inclined angle increases, both the length and recirculation heat of the recirculation zone below the arch increase and the ignition distance of the PA and pulverized-coal mixture shortens. The flame penetration depth and residence time of pulverized-coal particles increase, being favorable to increase the pulverized-coal burnout. The NO emission and average temperature at the furnace exit decrease. The optimal inclined angle is 25°, to improve the characteristics of pulverized-coal burnout, NO emission, and heat transfer without a tendency of slagging on the ash hopper walls. After retrofitting, the flame penetration depth increases and the flame center shifts downward. The boiler performance is improved with absolute increases of 3.55, 3.31, and 2.20% in boiler efficiencies and relative reductions of 28.65, 19.47, and 12.53% in NO emissions at 300, 240, and 190 MW, respectively.

Acknowledgment. The authors gratefully acknowledge financial support for this research from the National Natural Science Foundations of China (50806024 and 50721005) and the Hi-Tech Research and Development Program of China (863 Program) (Contract 2006AA05301).

Nomenclature

PA = primary air
VA = vent air
SA = secondary air
R_{90} = pulverized-coal fineness (%)
R and G = red and green data of color images
H = distance from the burner nozzle to the ash hopper top (m)
h = penetration depth of the arch-injected air in the lower furnace (m)
d = flame depth in the lower furnace (m)
T_{gas} = flue gas temperature (K)
$C_{p_{gas}}$ = specific heat capacity (kJ kg^{-1} K^{-1})
v_x = recirculation velocity (m/s)
ρ_{gas} = flue gas density (kg/m^3)
l = recirculation zone length (m)
λ = wavelength (nm)
α = mass fraction of the nitrogen release in the volatile
β = percentage of the nitrogen in the volatile evolving as a HCN intermediate